Electronic Supplementary Material (ESI) for Nanoscale.
This journal is © The Royal Society of Chemistry 2014

Bias Induced Transition from an Ohmic to a Non-Ohmic Interface in Supramolecular Tunneling Junctions with Ga_2O_3/EGaIn Top Electrode

Kim S. Wimbush,[1] Raluca M. Fratila,[1] Dandan Wang,[2] Cao Liang,[2] Li Yuan,[2] Qi Dongchen,[3] Nikolai Yakovlev,[3] Loh Kian Ping,[2,5] David N. Reinhoudt,[1] Aldrik Velders,[1,4]* Christian A. Nijhuis[2,3,5]*

[1] Laboratory of Supramolecular Chemistry and Technology, MESA+ Research Institute, University of Twente, 7500AE Enschede, The Netherlands

[2] Department of Chemistry, National University of Singapore, 3 Science Drive 3, Singapore 117543

[3] Interface of Materials Research and Engineering, 3 Research Link, Singapore, 117602

[4] BioNanoTechnology group, Wageningen University, PO Box 8038, 6700 EK Wageningen, The Netherlands

[5] Graphene Research Centre, National University of Singapore, 6 Science Drive 2, Singapore 117546

*corresponding authors:
Tel.: (+65) 6516 2667
e-mail: christian.nijhuis@nus.edu.sg
Tel: (+31) 317485970
e-mail: aldrik.velders@wur.nl

Nomenclature

The junctions are described in the text as follows: Au^{TS}-βCDSAM//X//Ga_2O_3/EGaIn where "Au^{TS}" is the template-stripped gold electrode, "-"represents the covalent interface of the Au^{TS} interacting with the sulfur of the heptathioether functionalized βCD, "X" represents the dendrimer, "Ga_2O_3" represents the surface layer of gallium oxides of gallium, "//" represents the non-covalent interfaces of i) the supramolecular host-guest interaction between the βCD and the terminal functional group of the dendrimer, and ii) the interface between the molecular structure and the Ga_2O_3 layer, and "/" indicates the interface of the bulk EGaIn with the surface layer of Ga_2O_3.[1-3]

Synthesis of Compounds

Preparation of heptathioether-functionalized β-cyclodextrin,[4, 5] G1-PPI-$(Ad)_4$,[6] G1-PPI-$(Fc)_4$[7] and G0-PAMAM-$(Fc)_4$[8] dendrimers was described previously. All compounds were characterized with nuclear magnetic resonance spectroscopy (^{1}H NMR) and mass spectrometry (MALDI ToF and ESI-MS). All compounds gave similar results to the previously published procedures. Eutectic alloy of gallium and indium was purchased from Aldrich and used as such.[3] The G0-PAMAM-$(EG\text{-}Ad)_4$ dendrimer was prepared as described below and shown in figure S1.

Synthesis and Characterization of Dendrimers G0-PAMAM-$(EG\text{-}Ad)_4$

Step 1: Synthesis of Ad-EG-N_3 (3)

11-Azido-3,6,9-trioxaundecan-1-amine (**2**) (1 mmol, 218 mg) was dissolved in dry dichloromethane (20 mL) and NEt_3 (2 mmol, 202 mg, 270 μL) was added. The solution was cooled to 0°C using an ice bath, and a solution of adamantane-carboxylic acid chloride (**1**)

(1.5 mmol, 299 mg in 20 mL of dry dichloromethane was added dropwise. The ice bath was removed and the reaction mixture was allowed to reach the room temperature and stirred overnight. After that time, the reaction mixture was washed with aqueous 0.1M HCl solution (3 × 25 mL), aqueous saturated $NaHCO_3$ (3 × 25 mL), and water (3 × 25 mL). The organic layer was dried over Mg SO_4 and the solvent was evaporated under reduced pressure. The crude reaction product was purified by flash column chromatography (silicagel, CH_2Cl_2/MeOH 90/10) and isolated as a colorless oil. Yield: 78% (0.78 mmol, 296 mg). ^{1}H NMR (600 MHz, $CDCl_3$) δ = 6.12 (bs, 1H, CON*H*), 3.68 (s, 8H, OC*H*$_2$C*H*$_2$OC*H*$_2$C*H*$_2$O) , 3.64 (m, 2H, OC*H*$_2$CH$_2$N$_3$), 3.55 (t, *J* = 5.0 Hz, 2H, NHCH$_2$C*H*$_2$O), 3.45 (q, *J* = 5.0 Hz, 2H, NHC*H*$_2$CH$_2$O), 3.40 (t, *J* = 5.0 Hz, 2H, OCH$_2$C*H*$_2$N$_3$), 2.04 (s, 3H, C*H*CH$_2$), 1.86 (s, 6H, CHC*H*$_2$CCONH), 1.72 (m, *J* = 15.5 Hz, 6H, CHC*H*$_2$CH). ^{13}C NMR (75 MHz, $CDCl_3$) δ = 178.3, 71.0, 70.8, 70.5, 70.3, 70.182, 50.9, 40.8, 39.4, 39.2, 36.8, 28.4. ESI-TOF Calculated for $C_{19}H_{32}N_4O_4$: *m/z* 380.1 Found: *m/z* 381.1 [M+H].

Step 2: Synthesis of Ad-EG-NH_2 (4)

Ad-EG-N_3 **(3)** (0.1 mmol, 38 mg) was dissolved in 20 mL of methanol, and Pd/C (0.01 eq, 0.01 mmol, 10 mg of 10% Pd/C) was added. Nitrogen was bubbled through the solution for 5 min, and then the reaction mixture was stirred at room temperature under H_2 (ambient pressure) for 30 min (monitored by TLC and IR spectroscopy – the disappearance of the characteristic azide peak at 2098 cm^{-1} – to assess the complete consumption of the starting material). The reaction mixture was filtered over a Celite pad, and the solvent was evaporated to afford the Ad-EG-NH_2 as a colorless oil, in (nearly) quantitative yield (> 95%, 0.1 mmol, 35 mg). The product was used in the next step without further purification. ^{1}H-NMR (300 MHz, $CDCl_3$): 6.25 (bd, 1H, CON*H*), 3.67-3.59 (m, 9H, OC*H*$_2$C*H*$_2$OC*H*$_2$C*H*$_2$O and OCH$_2$C*H*$_2$NH$_2$), 3.55 (m, 2H, NHCH$_2$C*H*$_2$O), 3.45 (q, *J* = 5.0 Hz, 2H, NHC*H*$_2$CH$_2$O),

2.87 (dm, 1H, $OCH_2CH_2NH_2$) 2.10 (bs, 2H, $OCH_2CH_2NH_2$) 2.04 (s, 3H, $CHCH_2$), 1.86 (s, 6H, $CHCH_2CCONH$), 1.72 (m, J = 14.9 Hz, 6H, $CHCH_2CH$). ^{13}C NMR (75 MHz, $CDCl_3$) δ = 185.4, 70.7, 70.5, 70.4, 70.2, 41.8, 40.8, 39.4, 39.2, 36.8, 29.9, 28.4, 28.3. ESI-TOF Calculated for $C_{19}H_{32}N_4O_4$: *m/z* 354.3 Found: *m/z* 355.3 [M+H].

Step 3: Synthesis of Ad-EG-NCS[9] (5)

A solution of Ad-EG-NH_2 **(4)** (30 mg, 0.085 mmol) in 5 mL of dichloromethane was prepared in a 25 mL round-bottomed flask equipped with a stir bar. The solution was then cooled to 0 °C with an external ice/brine bath. Saturated aqueous $NaHCO_3$ (5 mL) was added, and the biphasic mixture stirred vigorously (~500 rpm) for 5 min. The stirring was stopped, and thiophosgene (10 eq., 65μL) was added via syringe *to the organic layer*. The flask was sealed with a rubber septum, and immediately, vigorous stirring was restored, the reaction was removed from the ice bath, and allowed to stir for 30 min at room temperature. The layers were separated and the aqueous layer was extracted with CH_2Cl_2 (2 × 2 mL). The combined organics were dried over Na_2SO_4, filtered, and concentrated *in vacuo* to afford the crude isothiocyanate as a yellow oil. The isothiocyanate was used immediately in the subsequent step without any further purification. (32 mg, 0.08 mmol, 94%). ESI-TOF Calculated for $C_{20}H_{32}N_2O_4S$: *m/z* 396.2 Found: *m/z* 397.2 [M+H].

Step 4: Synthesis of G0-PAMAM-(EG-Ad)$_4$ (6)

A solution of Ad-EG-NCS **(5)** (24 mg, 0.06 mmol, 4.5 eq) in 5 mL of dry $CHCl_3$ was added to a solution of the amino-terminated G0-PAMAM dendrimer[1] (6.9 mg, 0.0133 mmol, 1eq) in 5 mL of dry $CHCl_3$. The reaction mixture was stirred at room temperature for

[1] The amino-terminated G0-PAMAM dendrimer (Sigma-Aldrich) is supplied as 20% wt solution in methanol; the complete removal of the methanol prior the coupling with the isothiocyanate is required in order to avoid the side reaction between MeOH and the Ad-EG-NCS.

48 h; after that time, the solvent was evaporated to afford the G0-PAMAM-EG-$(Ad)_4$ (26 mg, 0.0124 mmol, 93%).

^{1}H NMR (600 MHz, $CDCl_3$) $CD_3OD/CDCl_3$ 1/1 v/v) δ = 3.50 (m, 32H), 3.40 (m, 8H), 3.27-3.13 (24H), 2.73 (m, 8H), 2.64 (m, 8H), 2.58 (m, 8H), 2.35 (s, 4H), 2.22 (m, 8H), 1.89 (bs, 12H), 1.69 (s, 24H), 1.58 (m, 24H). ^{13}C NMR (151 MHz, CD_3OD) δ = 180.9, 175.3, 71.5, 71.3, 70.5, 52.3, 51.2, 42.4, 41.8, 40.1, 37.6, 34.6, 29.6.

Figure S1: Synthesis of dendrimers G0-PAMAM-$(EG\text{-}Ad)_4$

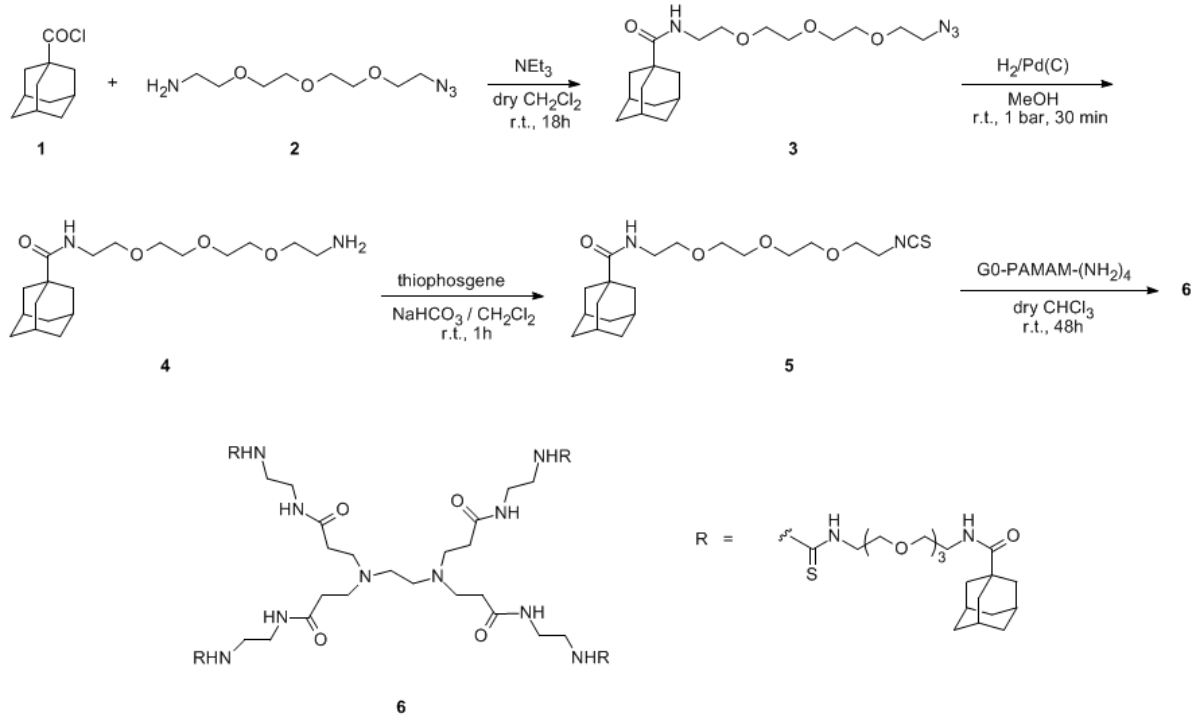

Preparation of Supramolecular Tunneling Junctions

Formation of the SAMs: Ultra flat substrates of thin gold metal films supported by a polymer coated glass slide were obtained by peeling of an evaporated gold film from a Si/SiO_2 template (the 'mechanical template-stripping' procedure (TS)) as previously described. The βCD SAMs were prepared by immersing freshly cleaved ultra-flat gold

substrates into a 0.1-1mM solution of βCD adsorbate (Fig. 1A) dissolved in ethanol for 16 h at 60°C. The substrates were removed and placed immediately in a vial of ethanol at 60°C for one to two minutes to avoid precipitation of the heptathioether-functionalized βCD. Subsequently, the substrates were rinsed with ethanol (room temperature) and MilliQ water, and then dried under a stream of dry nitrogen. As previously published,[1-3, 10] electrochemical impedance spectroscopy was used to characterize control βCD SAMs and yielded similar results.

Adsorption of the Dendrimer: We formed monolayers of the dendrimers on the βCD host-surface by following previously reported procedures by immersing the βCD SAMs on Au^{TS} in acidic (pH = 2) aqueous solutions of the dendrimers with a concentration of the end groups of 2.0 mM in the presence of 2.1 mM of native βCD for at least 1 h (Fig. 1H, I).[8, 11, 12] Subsequently the samples were rinsed with MilliQ water and dried under a stream of dry nitrogen. The assembly processes was followed with control samples by surface plasmon resonance (SPR) spectroscopy and the monolayers were characterized with cyclic voltammetry. The results were comparable to previously reported data.

Ga_2O_3/EGaIn top Electrode: The Ga_2O_3/EGaIn top contact was formed following previously reported procedures.[1-3] The resulting cone-shaped tip was carefully brought into contact with the Au^{TS} surface supporting the SAM. A wire directly attached to the metal needle on the syringe connected the Ga_2O_3/EGaIn electrode electrically with an electrometer (Keithley 6430). The Au substrate was grounded by means of a gold needle that penetrated the SAM and contacted the Au directly. A triaxial cable connected the two electrodes to an external amplifier. The electrometer applied a bias, V, across the junction. A positive value of V corresponded with EGaIn being biased positively with respect to the Au. The entire setup, except the source-meter was housed in a home-built aluminum Faraday cage.

J(*V*) measurements of Supramolecular Tunneling Junctions

For all *J*(V) measurements we selected junctions that had their electrical characteristics within one log-standard deviation from the log-mean of the current density at ±2.0 V. The *J*(V) traces (with one scan (*N*) = 0.0 V → + 2.0 V → 0.0 V → - 2.0 V → 0.0 V) were recorded in steps of 0.10 V, in both sweep directions, giving a total of 82 points for a single scan. The rectification ratio (*R*) was calculated for each of the individual scans using the equation $R = |J|(-2.0\ V)/|J|(+2.0\ V)$.

Voltage Cycling, Poly(propylene) Imine Dendrimers: Figure S2 shows the resulting value of rectification (*R*) defined as [$R = |J|(-2.0\ V)|/|J|(+2.0\ V)|$] as a function of voltage cycling (*N* = 100) in the range of ±2.0 V for the junctions, Au^{TS}-βCDSAM//G1-PPI-$(Fc)_4$//Ga_2O_3/EGaIn , Au^{TS}-βCDSAM//G1-PPI-$(Ad)_4$//Ga_2O_3/EGaIn and Au^{TS}-βCDSAM//Ga_2O_3/EGaIn. It can be seen that as the number of scans increase the value of *R* also increases for all supramolecular tunneling junctions, regardless of their molecular structure.

Figure S2: Semi-log plot of *R* Vs. Scan Number, for junctions Au^{TS}-βCDSAM//G1-PPI-$(Fc)_4$//Ga_2O_3/EGaIn, (—), Au^{TS}-βCDSAM//G1-PPI-$(Ad)_4$//Ga_2O_3/EGaIn (—) and Au^{TS}//βCDSAM//Ga_2O_3/EGaIn (—).

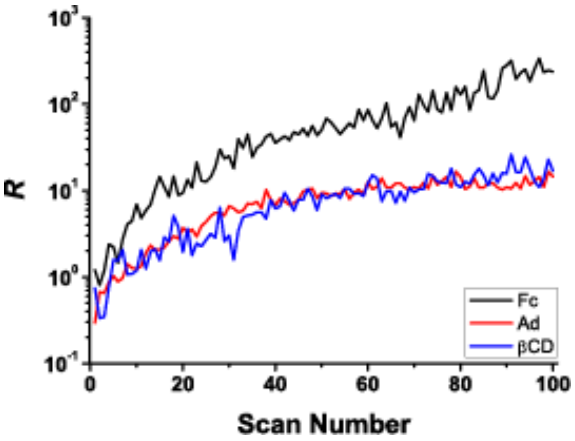

Voltage Pulse Vs. Time, Poly(propylene) Imine Dendrimers: The voltage pulse experiments were carried out as follows. First, four $J(V)$ scans were measured in the bias range of ±2.0 V to determine R at $t = 0$. A voltage pulse (V_{pulse}) was then applied at +1.0 V, +1.5 V, +2.0 V or +2.5 V with a total duration of 3600 s. To follow the change in the electrical characteristics of the junctions during this voltage pulse, we interrupted the voltage pulse to record five $J(V)$ scans at t = 120, 300, 600, 900, 1800, 2400 and 3600 s. R was calculated for each individual scan and then averaged using the arithmetic mean to give the final value of R. We choose to record five $J(V)$ traces, and not more, to determine the changes in R with, at least, normal-standard deviations rather than a single value of R, and to minimize the impact of these measurements on R, *vide supra*. To show the reproducibility of this trend, the measurements were carried out at least in duplicates across the three different supramolecular junctions of Au^{TS}-βCDSAM//G1-PPI-$(Fc)_4$//Ga_2O_3/EGaIn, Au^{TS}-βCDSAM//G1-PPI-$(Ad)_4$//Ga_2O_3/EGaIn and Au^{TS}-βCDSAM//Ga_2O_3/EGaIn (except for the measurements performed on junction Au^{TS}-βCDSAM//Ga_2O_3/EGaIn when holding at +1.5 V and +2.0V) (Fig. S3E). As shown, all supramolecular junctions displayed a similar increase in R for the applied voltage pulse and the value of R seems to increase exponentially as a function of V_{pulse} (Fig. S3). In some of the duplicate measurements there was a sharp uncharacteristic decrease in R with an increase in t, i.e., in Fig. S3A for V_{pulse} = 2.0 V (2) at t = 45 min. This is likely due to a small drift in the EGaIn tip during the two hour measuring period. The drift causes new areas of the Ga_2O_3/EGaIn tip that is unoxidized to be in contact with the SAM, thus decreasing R.

Figure S3: (A-E) Semi-log plot of the increase in rectification (*R*) [R = |*J*(-2.0 V)|/|*J*(+2.0 V)|] in the supramolecular tunneling junctions Au^{TS}-βCDSAM//G1-PPI-$(Fc)_4$//Ga_2O_3/EGaIn (A), Au^{TS}-βCDSAM//G1-PPI-$(Ad)_4$//Ga_2O_3/EGaIn (B,C) and Au^{TS}-βCDSAM//Ga_2O_3/EGaIn (D,E), as a function of V_{pulse} of +1.0 V (▼), +1.5 V (▲), +2.0 V (●), +2.5 V (■) measured at by performing five *J*(V) scans ±2.0 V at *t* = 120, 300, 600, 900, 1800, 2700, and 3600 s. (F) Semi-log plot of *R*(60) min vs. Applied Voltage Pulse, showing that *R* increases exponentially with V_{pulse}.

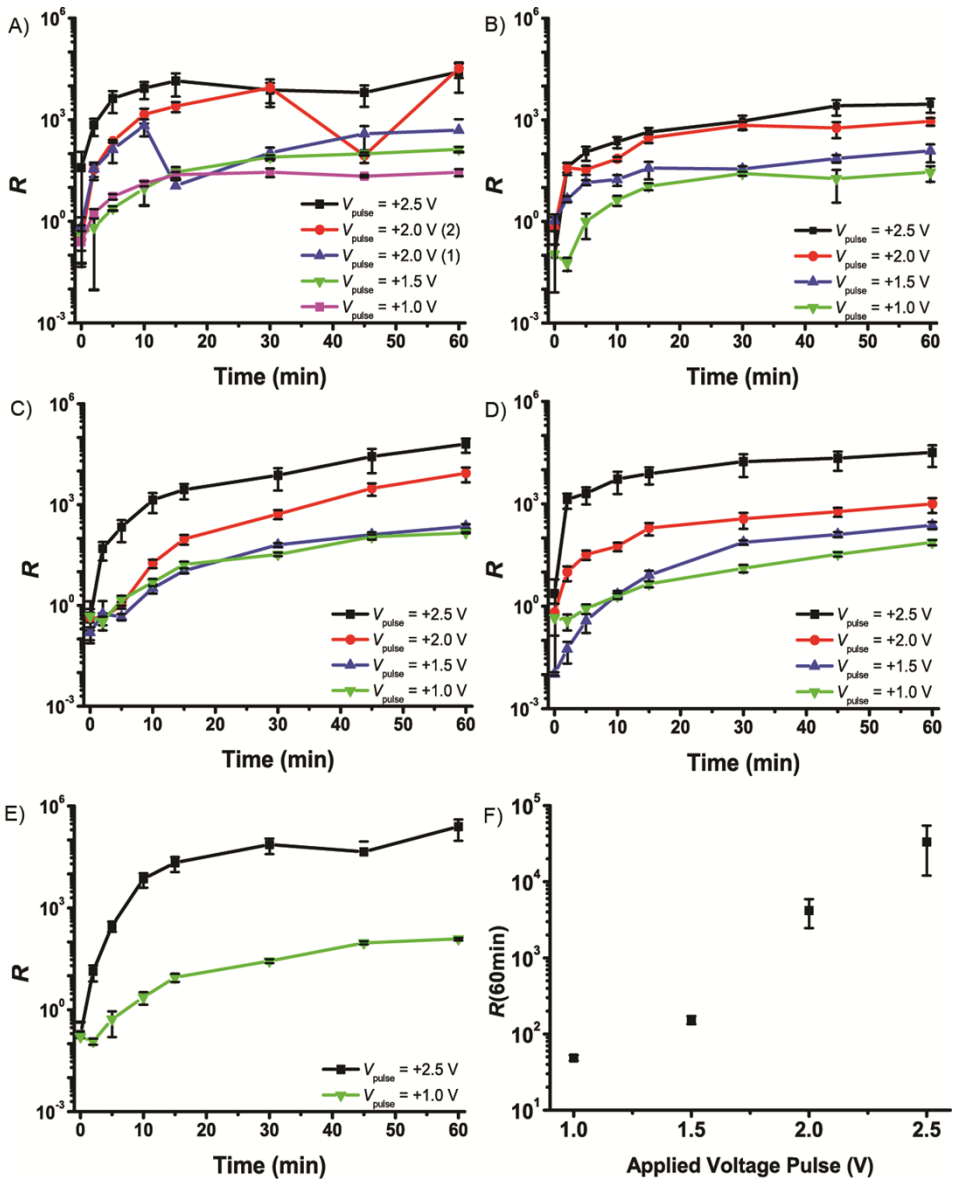

Single Voltage Pulse, Poly(propylene) Imine Dendrimers: The experiments, where a single voltage pulse was applied across the junction Au^{TS}-βCDSAM//G1-PPI-$(Fc)_4$//Ga_2O_3/EGaIn (Fig. 2B and D), were performed as follows. First, four $J(V)$ scans were recorded over a voltage range of ±2.0 V. We used scan number four to calculate the initial value of R which we defined for this experiment as the starting values. A voltage pulse was then applied at +2.0 V (Fig. 2B), or -2.0 V (Fig. 2D), for a period of 900 s and $|J|$ was measured at intervals of 0.10 s. An additional five $|J|(V)$ scans were then performed ±2.0 V and R was determined for each individual scan, and averaged to give the arithmetic mean of R. To test if the changes in the $J(V)$ characteristics were reversible (Fig. 3C), we applied across one junction of Au^{TS}-βCDSAM//G0-PPI-$(Fc)_4$//Ga_2O_3/EGaIn a V_{pulse} = +2.0 V for t = 600 s followed by a V_{pulse} = -2.0 V t = 1200 s and performed comparison $J(V)$ characteristic measurements ±2.0 V as described above. For the stability measurements (Fig. 3D), we applied across one junction of Au^{TS}-βCDSAM//G0-PPI-$(Fc)_4$//Ga_2O_3/EGaIn a V_{pulse} = + 2.5 V for t = 3600 s and measured the $J(V)$ characteristics ±2.0 V directly after V_{pulse} and again 16 hours later.

Voltage Cycling and Single Voltage Pulse, Poly(amido amine) Dendrimers: For the junctions of Au^{TS}-βCDSAM//G0-PAMAM-$(Ad)_4$//Ga_2O_3/EGaIn and Au^{TS}-βCDSAM//G0-PAMAM-EG-$(Ad)_4$//Ga_2O_3/EGaIn (Fig. 3B and Fig. S4, which were investigated to determine the effect that the dendritic core has on the $J(V)$ characteristics by changing the packing density of the dendrimer on the supramolecular printboard and the orientation of the terminal functional moieties of the dendrimers, (Table 1)[4, 5, 8, 11, 12] first 20 $J(V)$ scans were recorded over a range of voltages of ± 2.0 V (Fig. S4, ■). This was followed by a V_{pulse} = +2.5 V of t = 300 s, after which five more $J(V)$ scans were recorded over a range of voltages of ± 2.0 V (Fig. S4, ●) In a similar manner to all other tunneling junctions which had a V_{pulse} applied, after the V_{pulse}, the $|J|(V)$ scan displayed larger values of $|J|$ at - 2.0 V,

and smaller values of $|J|$ at + 2.0 V than before V_{pulse}. In other words, the rectification ratio increased (Fig. 3B). Therefore, after changing the dendrimer core, the number of interactions of the dendrimers with the host surface, and the surface coverage of the dendrimers with the host surface, an increase in the value of R is still observed after applying a V_{pulse}. These results indicate that the increase of the value of R is independent of the chemical and supramolecular structure of the SAMs in the tunneling junctions.

Figure S4: Molecular structure for the dendritic core of the generation 0 poly(amido amine) dendrimer (PAMAM) (A) which is functionalized with adamantyl (Ad) (B) or Ad with a tetra-ethylene glycol (EG) tether (C). Schematic of the orientation of the dendrimers binding to the supramolecular platform; G0-PAMAM-$(Ad)_4$ binds with three out of four terminal moieties (D), whilst G0-PAMAM-EG-$(Ad)_4$ binds with all four (E). Semi-log plots of $|J|(V)$ scans measured ±2.0 V, 20 scans measured before (■) and 5 scans after (●) being subjected to V_{pulse} = +2.5 V for t = 300 s, for junctions Au^{TS}-βCDSAM//G0-PAMAM-$(Ad)_4$//Ga_2O_3/EGaIn (F) and Au^{TS}-βCDSAM//G0-PAMAM-$(EG\text{-}Ad)_4$//Ga_2O_3/EGaIn (G).

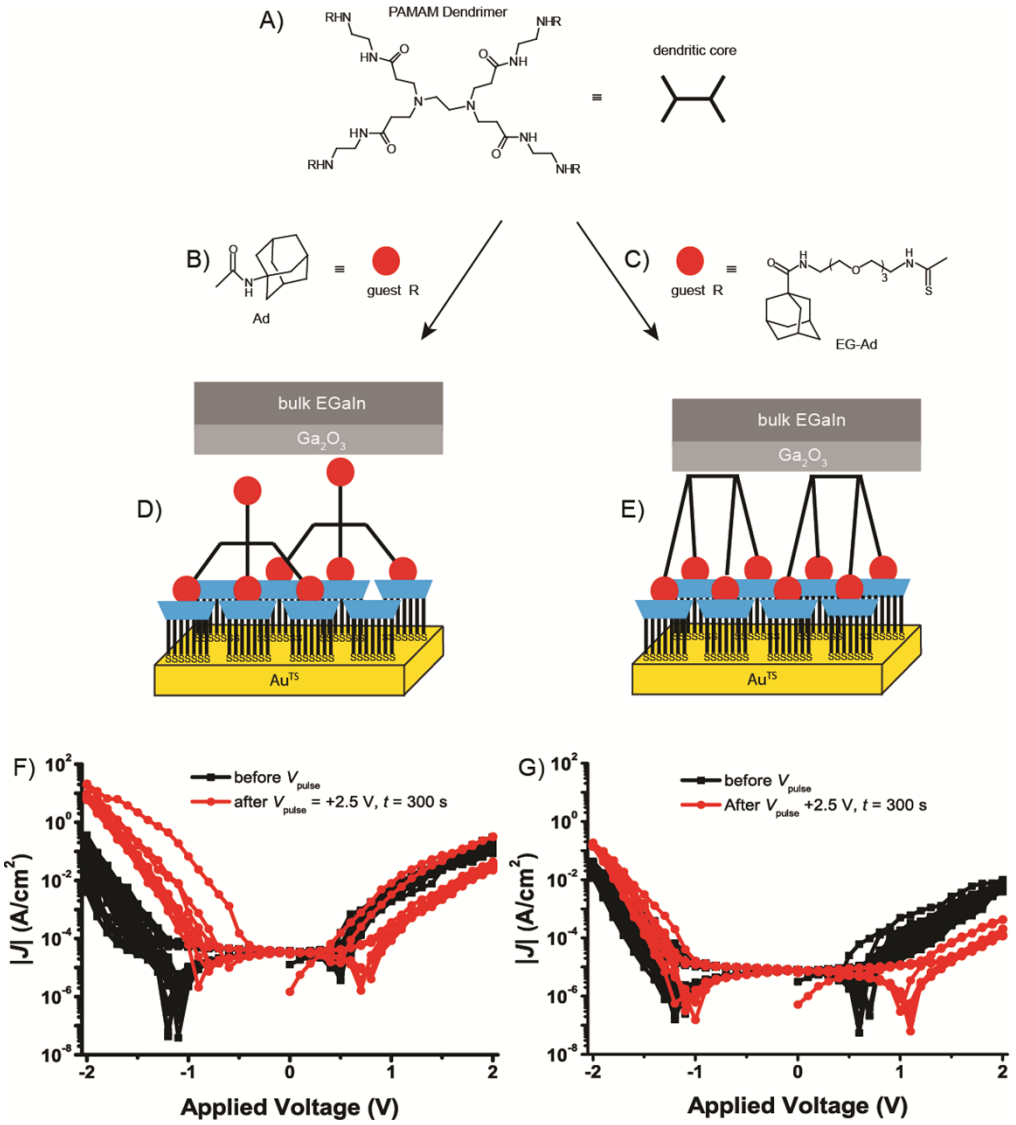

J(*V*) Characteristics of Oxidized Ga_2O_3/EGaIn tips

Due to the liquid nature of the Ga_2O_3/EGaIn top-electrode, two methods were used to oxidize the tip and to minimize mechanical stress and vibrations to ensure the oxide layer remains undamaged during the handling and measurements. In one method the Ga_2O_3/EGaIn tip was oxidized whilst suspended in air using the same electrometer as was used to measure the electrical characteristics of the tunneling junctions by simply applying a bias to the tip of Ga_2O_3/EGaIn of 50 V for 2 or 4 hours while the Au^{TS} was grounded. Subsequently, *J*(V) curves were measured of junctions of the oxidized Ga_2O_3/EGaIn tips directly in contact with Au^{TS}, i.e., a junction of Au^{TS}//Ga_2O_3/EGaIn. Another method for oxidizing the tip was to electrochemically oxidize the Ga_2O_3/EGaIn. After forming a

Ga_2O_3/EGaIn tip by the steps described earlier, this tip was immersed into a beaker with 50 mL of water using the micromanipulator with Pt as the counter electrode. The Ga_2O_3/EGaIn tip was biased from 0 to 1.0 V back to 0 V using an electrometer (Keithley). The tip was allowed to dry under ambient conditions overnight and then brought into contact with bare Au^{TS} to form the junction Au^{TS}/Ga_2O_3/EGaIn. Thus in this experiment, the syringe with a suspended Ga_2O_3/EGaIn tip was not removed from the micromanipulator. For both oxidized tips, the *J*(V) curves were measured by grounding the bottom Au^{TS} electrode and biasing the Ga_2O_3/EGaIn top electrode with the air oxidized tip gave a value of *R* of 4.5 × 10^3 at ±5.0 V (Fig. 5A, B) whilst the electrochemically oxidized tip gave an *R* value of 2.2 × 10^2 at ±1.5 V (Fig. S5).

Figure S5: (A) Semi-log plot of averaged |*J*|(*V*) measurements performed ±1.5 V on junctions of Au^{TS}//Ga_2O_3EGaIn. (B) Histogram of log rectification ratio (*R*), where *R* = |*J*(-1.5 V)|/|*J*(+1.5 V)|.

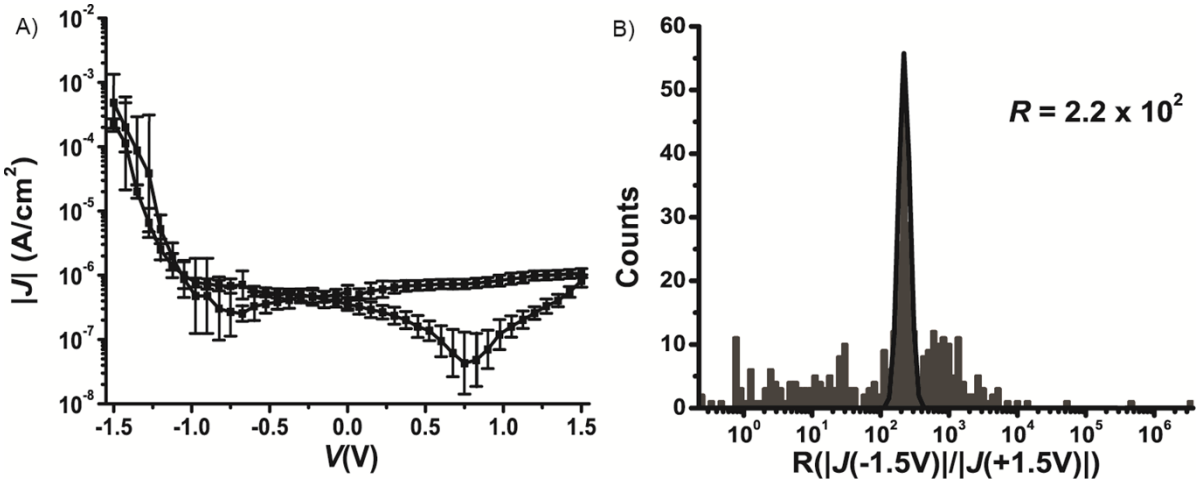

Kelvin Probe Microscopy

The work function of bulk EGaIn is measured by Scanning Kelvin Probe Microscopy on a Park XE-100 AFM system. The AFM is working on amplitude-modulated non-contact mode

with the phase signal used as the feedback. To get the surface potential signal (work function), an external lock-in amplifier is connected to the XE-100 system. During the measurements, an AC bias of frequency ω (V_{AC}sinωt) is applied to the conductive AFM tip, in addition to the DC voltage (V_{DC}) from the DC bias feedback control loop. The resulting electrostatic force between the tip and the sample, which is separated by external lock-in, can be calculated as

$$2 \times \left(\frac{C}{d}\right) \times (V_{DC} - V_S) \times V_{AC} sin\omega t,$$

in which C, d, V_S are equivalent capacitance, tip-to-surface distance and surface potential respectively. By zeroing the electrostatic force using the DC bias feedback loop, V_S can be acquired locally on a raster scanning fashion.

Photoelectron Spectroscopy

X-ray photoelectron spectroscopy (XPS) surface mapping of SAMs: We formed a junction of the form Au^{TS}-βCDSAM//Ga_2O_3/EGaIn with a cone-shaped tip of Ga_2O_3/EGaIn as described above and subsequently applied a V_{pulse} of +2.5 V for t = 900 s. Upon completion of the V_{pulse}, the junction was dissembled by lifting the cone-shaped Ga_2O_3/EGaIn electrode, exposing the βCD SAM that had previously been embedded in the Au^{TS}-βCDSAM//Ga_2O_3/EGaIn junction. The XPS mapping experiments were carried out on areas where the βCD SAM had been biased and were compared to areas that had not been biased. The XPS mapping of the C_{1s} and S_{2p} signals were performed using a Physical Electronics Quantera Scanning X-ray Microprobe instrument, equipped with a monochromatic X-ray source (Al Kα 1486.6 eV, 25 W with a beam size of 100μm), at ~ 5 e^{-8} torr and a detector angle of 45°. The C_{1s} peak at 284.8 eV was taken as the reference.

X-ray and Ultra-violet photoelectron spectroscopy (XPS and UPS): Two samples were prepared by placing large drops (with a surface area of ~1cm^2) of fresh Ga_2O_3/EGaIn on Au^{TS}. One sample was used directly to give 'native EGaIn', whilst 50 V was applied to the other sample for 4h in air using the electrometer to give 'oxidized EGaIn' The photoelectron spectroscopy measurements were carried out using A1 K_α x-ray radiation (hv = 1486.6eV) under ultra-high vacuum(UHV) conditions (base pressure 5×10^{-10} mbar) at room temperature using VG ESCALAB 220I-XL. Through calibration with Ni foil, all the spectra were normalized by the photon current. The work function was measured using 21.2 eV photon energy with a 5.0 V bias applied to the sample to overcome the work function of analyzer. The XPS data (Ga 3d spectra, Fig. 5 and Ga 2p spectra, Fig. S6) were fitted using a Shirley background and mixed Gaussian–Lorentzian functions following previously described procedures.[13] Quantitative analysis of the thickness of the gallium oxide was estimated from the fits to the spectra (using the Ga 3d spectra, Fig. 5) and based on the known thickness of the gallium oxide layer for the native EGaIn (~0.7 nm) following a previously described procedure (see below).

Table S1 shows the comparison of the atomic percentages of the Ga metal (G^0 (2p/3d)) and the Ga oxide/suboxide (Ga^{3+} + Ga^+ (2p/3d) for both the native and oxidized EGaIn samples. The relative ratio of the oxide and metal signal intensities are consistent with the ratio of the Ga 3d photoelectron spectra.

To calculate the thickness of the oxide layer (d_{ox}) we adapted previous published methods.[14-18] The thin film thickness was calculated from[14-16]

$$d_{ox} = \lambda_{ox} \sin\theta \ln \frac{I_{ox}}{\beta_1 I_{Metal}} + 1 \qquad (1)$$

where θ is the take-off angle, which was 90° in this measurement and I_{ox}/I_{metal} is ratio of the intensities of the oxide and metal signal, which can be calculated from the area under the

peaks of the Ga_2O_3 and the Ga metal in the fitted XPS spectra. λ_{ox} is the electron's inelastic mean free path (IMFP) in the oxide layer, which can be obtained from[17, 18]

$$\lambda_{ox} = E/[{E_p}^2 \beta_2 \ln(\gamma E)] \text{ Å} \quad (2)$$

where

$$E_p = 28.8(N_v \rho/A)^{1/2} \quad (3)$$

$$\beta_2 = -2.52 \times 10^{-2} + 1.05/({E_p}^2 + {E_g}^2)^{1/2} + 8.10 \times 10^{-4}\rho \quad (4)$$

$$\gamma = 0.151 p^{-0.49} \quad (5)$$

where E_p is the free electron plasmon energy. The parameters of E (kinetic energy) N_v (number of valence electrons), ρ (the density), A (molecular mass) and E_g (electron band gap) are all known for Ga_2O_3, and are 1463.5 eV, 24, 5.9 g/cm^3, 187.4 g/mol and 4.9 eV, respectively, allowing for the calculation of λ_{ox} = 24.5 Å. Both the native and oxidized Ga_2O_3/EGaIn samples contain an oxide layer, but their thickness is different. As the native Ga_2O_3/EGaIn sample has an oxide layer thickness 0.7nm, then from the above calculation the thickness for oxidized Ga_2O_3/EGaIn sample would be 1.2 nm.

Figure S6: High resolution XPS spectrum of the Ga2p region for native (A) and oxidized (B) Ga_2O_3/EGaIn samples

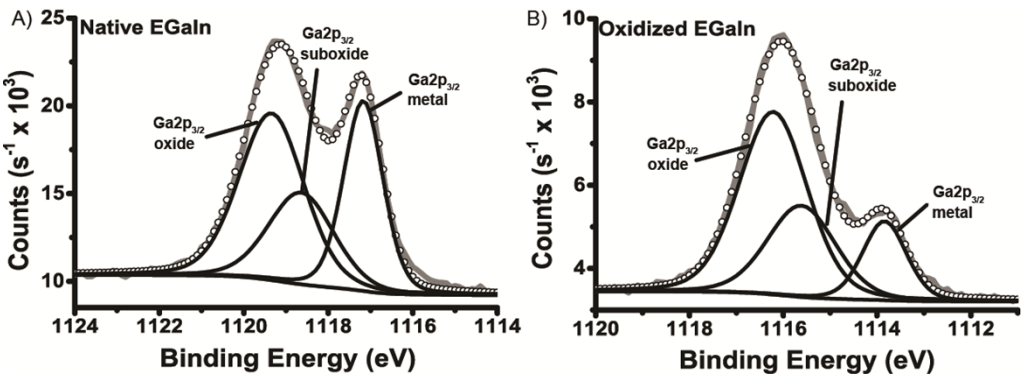

Table S1: Comparison of the atomic percentages of the Ga metal (G^0 (2p/3d)) and the Ga oxide/suboxide (Ga^{3+} + Ga^+ (2p/3d).

	Ga^0 (2p/3d)	**Ga^{3+} + Ga^{1+} (2p/3d)**
Native EGaIn	31%/64%	69%/36%
Oxide EGaIn	16%/50%	84%/50%

Ellipsometry Measurements

As the measurements required flat Ga_2O_3/EGaIn surfaces, thin films (~ 50 μm) of Ga_2O_3/EGaIn were made by squeezing two Au^{TS} substrates with drops of Ga_2O_3/EGaIn against each other several times (Fig. S7). After forming two flat native EGaIn surfaces, one surface was oxidized by using an electrometer to apply 50V for 2h, therefore giving one native Ga_2O_3/EGaIn and one oxidized Ga_2O_3/EGaIn sample. Variable angle spectroscopic ellipsometry (VASE) was performed with an incident angle from 60°-85°, and a wavelength from 300 nm - 800 nm.

The fitting procedure of the ellipsometry data for the native EGaIn oxide layer is based on the library model of ITO (refractive index n = 2.32, extinction coefficient k = 0.17 at $\lambda =$ 800 nm) and the known thickness of the native EGaIn oxide layer (0.7 nm). This gives the experimental refractive index for the native EGaIn oxide layer (n = 2.43, k = 7.08 at $\lambda =$ 800 nm), which in turn allows for the fitting of the oxidized EGaIn data. The raw data and the fitted data are plotted in Figure S8. Compared to the reported refractive index for the bulk gallium oxide (where n is around 1.9),[19, 20] our refractive index is slightly higher, which may be due to the underlying liquid metal layer. From this measurement the oxide layer thickness of the native and oxidized EGaIn was found to be 0.2 nm and 2.3 nm, respectively. (Table S2). This gives an increase in the thickness of the oxide layer of 2.1 nm after oxidation.

Figure S7: Photographic images of the thin films (~ 50 μm) of Ga_2O_3/EGaIn on Au^{TS} made for the ellipsometry measurements.

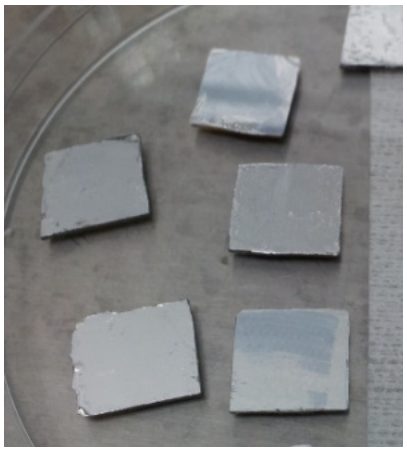

Figure S8: Ellipsometry measurements performed on oxidized (A) and native (b) Ga_2O_3/EGaIn samples. The solid lines represent the experimental data, and the dashed lines represent the fitted data.

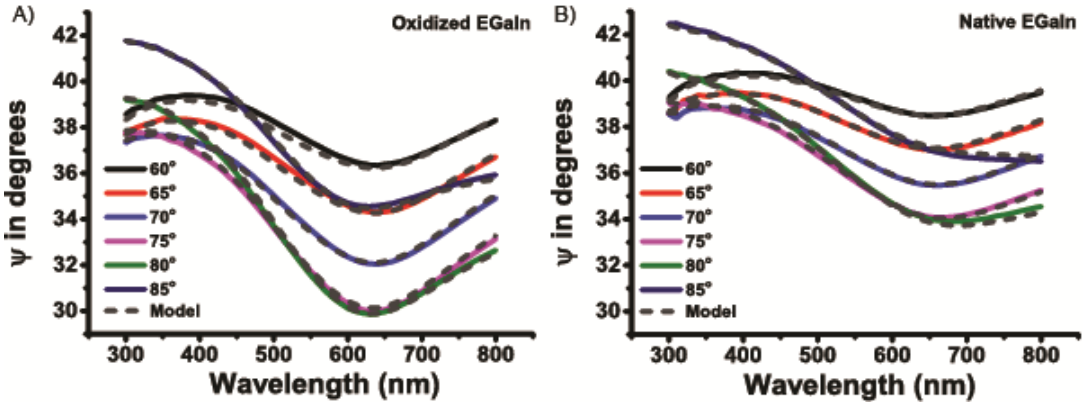

Table S2: Thickness of the oxide layer of the native and oxidized Ga_2O_3/EGaIn samples calculated from the ellipsometry measurements.

Sample Name	Thickness (nm)	Mean Square Area	Average thickness (nm)
Native EGaIn on Au^{TS}-1	0.39	0.7158	0.20
Native EGaIn on Au^{TS}-2	0	0.8528	
Oxidized EGaIn on Au^{TS}-1	2.58	4.045	2.32
Oxidized EGaIn on Au^{TS}-2	2.06	3.176	
Sample Name	**Thickness (nm)**	**Mean Square Area**	**Average thickness (nm)**
Native EGaIn on Au^{TS}-1	0.39	0.7158	0.20
Native EGaIn on Au^{TS}-2	0	0.8528	
Oxidized EGaIn on Au^{TS}-1	2.58	4.045	2.32
Oxidized EGaIn on Au^{TS}-2	2.06	3.176	

References

1. Chiechi, R. C.; Weiss, E. A.; Dickey, M. D.; Whitesides, G. M., Eutectic Gallium-Indium (EGaIn): A Moldable Liquid Metal for Electrical Characterization of Self-Assembled Monolayers13. *Angew. Chem., Int. Ed.* **2008**, 47, 142-144.
2. Nijhuis, C. A.; Reus, W. F.; Whitesides, G. M., Molecular Rectification in Metal-SAM-Metal Oxide-Metal Junctions. *J. Am. Chem. Soc.* **2009**, 131, 17814-17827.
3. Wimbush, K. S.; Reus, W. F.; van der Wiel, W. G.; Reinhoudt, D. N.; Whitesides, G. M.; Nijhuis, C. A.; Velders, A. H., Control over Rectification in Supramolecular Tunneling Junctions. *Angew. Chem. Int. Ed.* **2010**, 49, 10176-10180.
4. Beulen, M. W. J.; Bugler, J.; Lammerink, B.; Geurts, F. A. J.; Biemond, E. M. E. F.; van Leerdam, K. G. C.; van Veggel, F. C. J. M.; Engbersen, J. F. J.; Reinhoudt, D. N., Self-Assembled Monolayers of Heptapodant β-Cyclodextrins on Gold. *Langmuir* **1998**, 14, 6424-6429.
5. Beulen, M. W. J.; Bügler, J.; de Jong, M. R.; Lammerink, B.; Huskens, J.; Schönherr, H.; Vancso, G. J.; Boukamp, B. A.; Wieder, H.; Offenhäuser, A.; Knol, W.; van Veggel, F. C. J. M.; Reinhoudt, D. N., Host-Guest Interactions at Self-Assembled Monolayers of Cyclodextrins on Gold. *Chem. Eur. J.* **2000**, 6, 1176-1183.
6. Baars, M.; Karlsson, A. J.; Sorokin, V.; de Waal, B. F. W.; Meijer, E. W., Supramolecular Modification of the Periphery of Dendrimers Resulting in Rigidity and Functionality. *Angew. Chem., Int. Ed.* **2000**, 39, 4262-4265.
7. Cuadrado, I.; Moran, M.; Casado, C. M.; Alonso, B.; Lobete, F.; Garcia, B.; Ibisate, M.; Losada, J., Ferrocenyl-Functionalized Poly(propylenimine) Dendrimers. *Organometallics* **1996**, 15, 5278-5280.
8. Nijhuis, C. A.; Yu, F.; Knoll, W.; Huskens, J.; Reinhoudt, D. N., Multivalent Dendrimers at Molecular Printboards: Influence of Dendrimer Structure on Binding Strength and Stoichiometry and Their Electrochemically Induced Desorption. *Langmuir* **2005**, 21, 7866-7876.
9. Raheem, I. T.; Thiara, P. S.; Jacobsen, E. N., Regio- and Enantioselective Catalytic Cyclization of Pyrroles onto N-Acyliminium Ions. *Organic Letters* **2008**, 10, 1577-1580.
10. Gao, D. Q.; Scholz, F.; Nothofer, H. G.; Ford, W. E.; Scherf, U.; Wessels, J. M.; Yasuda, A.; von Wrochem, F., Fabrication of Asymmetric Molecular Junctions by the Oriented Assembly of Dithiocarbamate Rectifiers. *J. Am. Chem. Soc.* **2011**, 133, 5921-5930.
11. Huskens, J.; Deij, M. A.; Reinhoudt, D. N., Attachment of Molecules at a Molecular Printboard by Multiple Host-Guest Interactions. *Angew. Chem., Int. Ed.* **2002**, 41, 4467-4471.
12. Nijhuis, C. A.; Huskens, J.; Reinhoudt, D. N., Binding Control and Stoichiometry of Ferrocenyl Dendrimers at a Molecular Printboard. *J. Am. Chem. Soc.* **2004**, 126, 12266-12267.
13. Cademartiri, L.; Thuo, M. M.; Nijhuis, C. A.; Reus, W. F.; Tricard, S.; Barber, J. R.; Sodhi, R. N. S.; Brodersen, P.; Kim, C.; Chiechi, R. C.; Whitesides, G. M., Electrical Resistance of Ag^{TS}-$S(CH_2)_{n-1}CH_3$//Ga_2O_3/EGaln Tunneling Junctions. *J. Phys. Chem. C* 2012, **116**, 10848-10860.
14. Geng, S.; Zhang, S.; Onishi, H., XPS Applications in Thin Films Research. *Mater. Technol.* **2002**, 17, 234-240.
15. Mitchell, D. F.; Clark, K. B.; Bardwell, J. A.; Lennard, W. N.; Massoumi, G. R.; Mitchell, I. V., Film Thickness Measurements of SiO_2 by XPS. *Surf. Interface Anal.* **1994**, 21, 44-50.
16. Hochella, M. F.; Carim, A. H., A Reassessment of Electron-Escape Depths in Silicon and Thermally Grown Silicon Dioxide Thin-Films. *Surf. Sci.* 1988, 197, L260-L268.
17. Scharmann, F.; Cherkashinin, G.; Breternitz, V.; Knedlik, C.; Hartung, G.; Weber, T.; Schaefer, J. A., Viscosity Effect on GaInSn Studied by XPS. *Surf. Interface Anal.* **2004**, 36, 981-985.
18. Tanuma, S.; Powell, C. J.; Penn, D. R., Calculations of Electron Inelastic Mean Free Paths For 31 Materials. *Surf. Interface Anal.* **1988**, 11, 577-589.
19. Rebien, M.; Henrion, W.; Hong, M.; Mannaerts, J. P.; Fleischer, M., Optical Properties of Gallium Oxide Thin Films. *Appl. Phys. Lett.* **2002**, 81, 250-252.
20. Shan, F. K.; Liu, G. X.; Lee, W. J.; Lee, G. H.; Kim, I. S.; Shin, B. C., Structural, Electrical, and Optical Properties of Transparent Gallium Oxide Thin Films Grown by Plasma-Enhanced Atomic Layer Deposition. *J. Appl. Phys.* **2005**, 98.